

Influence of high energy milling on titanium oxide Ti_3O_5 crystal structure

Albina A. Valeeva^{1,a}, Irina B. Dorosheva^{2,3,b}, Anna A. Sushnikova^{3,c}¹Institute of Solid State Chemistry, Ural Branch of the Russian Academy of Sciences, 620108, Ekaterinburg, Russia²Ural Federal University, 620002, Ekaterinburg, Russia³Institute of Metallurgy, Ural Branch of the Russian Academy of Sciences, 620016 Ekaterinburg, Russia^aanibla.v@mail.ru, ^bdorosheva1993@mail.ru, ^csushnikova.ann@gmail.comCorresponding author: Albina A. Valeeva, anibla.v@mail.ru

PACS 71.20.Be, 81.07.Wx, 74.62.Bf, 61.05.C-, 68.37.Hk

ABSTRACT The titanium oxide (Ti_3O_5) microcrystals were synthesized by using solid-phase sintering from a mixture of titanium Ti and titanium dioxide TiO_2 powders. Subsequently, Ti_3O_5 nanocrystals were produced by using high-energy ball milling for 15 – 480 minutes. A full-profile analysis of the X-ray diffraction spectra of milled Ti_3O_5 powders showed that high-energy milling does not lead to disordering or changing of the structure and stoichiometry, the structure remains monoclinic (sp. gr. $C2/m$), and XRD reflections are broadened due to the small particle size and microdeformations. Experimental data show that increasing of the milling time leads to decreasing of the coherent scattering regions up to 26 nm, increasing of the powder volume fraction of the nanophase up to 81 %, and increasing of microdeformations value. The morphology and the surface area of milled nanopowders were examined by SEM, HRTEM and BET techniques.

KEYWORDS high-energy ball milling, Ti_3O_5 , XRD, BET, SEM, HRTEM**ACKNOWLEDGEMENTS** The work was carried out in accordance with the state assignment for the Institute of Solid State Chemistry of the Ural Branch of the Russian Academy of Science (No. 0397-2019-0001). Authors thanks to Gerasimov E. Yu. for HRTEM experiments.**FOR CITATION** Valeeva A.A., Dorosheva I.B., Sushnikova A.A. Influence of high energy milling on titanium oxide Ti_3O_5 crystal structure. *Nanosystems: Phys. Chem. Math.*, 2023, **14** (1), 107–111.

1. Introduction

The Ti–O system is attractive from both fundamental and applied points of view [1–6]. Well known due to its unique properties, titanium dioxide is the most studied material in wide areas of science and industry, ranging from memristors and capacitors to photocatalysts and photosorbents [7–10]. Nanoparticles of this material are synthesized mainly by bottom-up methods, namely, the sol-gel method, hydrothermal, anodizing, etc. [11–14]. In practical application, one of the disadvantages of this system is very wide band gap. A way to change the properties of this material is to introduce defects into the structure and Ti^{2+} and Ti^{3+} ions, which will lead to a change in the structure and properties [15–17]. Currently, a search is underway for materials that can be easily synthesized, have certain functional properties and structure, are stable during the entire period of operation under extreme conditions, and do not require additional energy supply [18]. One of the effective methods for obtaining nanoparticles is high-energy milling, which makes it possible to control the size of the resulting particles, dope the material during milling, and use various media for synthesis [19]. The milling of titanium oxides Ti_2O_3 [20, 21], TiO_2 (rutile) [22, 23] by means of high-energy ball milling leads to a decrease of the particle size only, the milling of ordered titanium monoxide TiO_y leads to a decrease of long-range order parameter of monoclinic TiO_y [24, 25], and phase transitions in TiO_2 from anatase to the high-pressure phase TiO_2 (II) occurs during milling [26, 27].

In this regard, the aim of this work is to obtain titanium oxide Ti_3O_5 nanoparticles with different particle sizes by varying the duration of high-energy milling and analyze the effect of high mechanical load on the morphology, crystal structure and stability of monoclinic phase of Ti_3O_5 under the intensive mechanical treatment.

2. Experiment

Initial microcrystals of titanium oxide Ti_3O_5 with an average size of about 30 μm were synthesized by solid-phase sintering from a mixture of titanium (Ti) and titanium dioxide (TiO_2) powders in a vacuum of 10^{-3} Pa at 1770 K. Ti_3O_5 nanoparticles with different particle sizes were obtained by high-energy milling of microcrystals in a Retsch PM 200 planetary ball mill. To minimize sample contamination during milling, ZrO_2 stabilized with Y_2O_3 was chosen as the material for the milling bowls and balls. The optimal mass ratio of milling balls and Ti_3O_5 powders, namely 10 : 1, was

chosen to effectively obtain the smallest nanoparticle size. Isopropyl alcohol was used as the milling liquid; the speed of rotation of the support disk was 500 rpm with the duration of milling 15, 30, 60, 120, 240 and 480 min.

Crystal structure studies of the initial and milled titanium oxide powders Ti_3O_5 were performed in $\text{CuK}\alpha_{1,2}$ radiation using XRD-7000 (Shimadzu, Japan) autodiffractometer. The X-ray diffraction patterns (XRD) were taken in the step-by-step scanning mode with $\Delta(2\theta) = 0.02^\circ$ in the range of 2θ angles from 10° to 140° with high statistics. The pseudo-Voigt function was used for a full-profile description of X-ray diffraction reflections:

$$V(\theta) = c \cdot a \left[1 + \frac{(\theta - \theta_0)^2}{\theta_L^2} \right]^{-1} + (1 - c) \cdot a \cdot \exp \left[-\frac{(\theta - \theta_0)^2}{2\theta_G^2} \right], \quad (1)$$

where c is the relative contribution of the Lorentz function to reflection intensity; θ_L and θ_G are the Lorentz and Gaussian functions parameters, respectively; a is the normalizing intensity factor; θ_0 is the maximum position of the function and reflection.

The dimensional and deformation contributions to the reflection broadening were determined by the Williamson–Hall method [28]. The reduced broadening was calculated by the formula:

$$\beta^*(2\theta) = \beta(2\theta) \frac{\cos\theta}{\lambda}.$$

The experimentally measured broadening $\beta(2\theta)$ is a superposition of the dimensional β_s and deformation β_d broadening according to the formula:

$$\beta = \sqrt{\beta_s^2 + \beta_d^2}.$$

The size of coherent scattering regions (CSR) was determined by the formula:

$$\langle D \rangle = \frac{1}{\beta^*} \quad (2\theta = 0).$$

The morphology of the synthesized and milled powders were examined on Ultra 55 (Carl Zeiss, Germany) scanning electron microscope (SEM) under high vacuum. The working distance (WD) was 7.5 – 10 mm, the electron high tension (EHT) was 20 – 25 kV. In order to avoid excessive electrization of powder during electron microscope imaging, the examined powder was deposited on a conducting adhesive tape from carbon. The structure of the milled powders was studied by using the high-resolution transmission electron microscopy (HRTEM) on a JEM 2010 electron microscope (JEOL, Japan) with accelerating voltage of 200 kV and ultimate lattice resolution of 140 pm. Imaging was performed by means of CCD matrix of Soft Imaging System (Germany). The device was equipped with a Phoenix (EDAX, USA) energy-dispersive characteristic X-ray radiation (EDX) spectrometer with a semiconducting Si(Li)-detector with energy resolution of 130 eV. For HRTEM experiments Ti_3O_5 particles were placed into alcohol and were further deposited on perforated carbon substrates (diameter of holes of about 1 μm) fixed on copper grids. Particles were deposited with the use of a UZD-1UCh2 ultrasonic disperser, which allowed uniform particle distribution on the substrate surface. After the grids were extracted from alcohol, the alcohol was evaporated. The specific surface area (SSA) of the powders was measured using Gemini VII 2390 (Micromeritics, USA) analyser implementing the Brunauer–Emmett–Teller (BET) method with preliminary degassing at 120°C .

3. Results and discussion

Figure 1 shows X-ray diffraction patterns of the initial and milled powders of titanium oxides Ti_3O_5 for 15 to 480 min. Detailed analysis of XRD patterns of ball milled Ti_3O_5 (Fig. 1) showed that the crystal structure of nanocrystal powder coincides with the crystal structure of microcrystal powder Ti_3O_5 , i.e. the monoclinic structure of Ti_3O_5 (sp. gr. $C2/m$, PDF Number: 11-217) is highly stable with respect to high-energy milling, and fragmentation does not lead to changing of crystal symmetry.

The XRD patterns of milled titanium oxide show broadening of the reflections associated with the small grain size and the microdeformations in the system due to high-energy milling. The dimensional and deformation contributions to the reflection broadening were determined by the Williamson–Hall method. The full-profile analysis of X-ray diffraction reflections showed that ball milling leads to a decrease in the coherent scattering region (CSR) from 30 μm to 26 nm, an increase in microdeformations from 0.02 % for initial powder to 0.49 % for the milled one.

The nanofraction volume of the Ti_3O_5 powders after high-energy milling at different durations showed an increase in the content of the nanosized powder phase from 1 to 81 % and decreasing of CSR with an increase in the milling time from 15 to 480 min (Table 1). Measurements of the specific surface areas of the initial Ti_3O_5 powders and ball milled powder for 480 min show the significant increasing of the SSA values from 0.1 to 17 m^2/g , respectively (Table 1).

Figure 2 shows SEM images of the initial and ball milled Ti_3O_5 powders obtained by high-energy milling. The size of the initial microcrystals is 10 – 30 μm . The shape of the microcrystals is complex, at higher magnification one can observe the layering of the structure, steps and terraces are visible. Analysis of SEM images showed that milling for 480 min leads to fragmentation of particles, nanocrystals with size about 25 – 50 nm are observed, nanocrystals stick to each other and form agglomerates up to 1 μm in size.

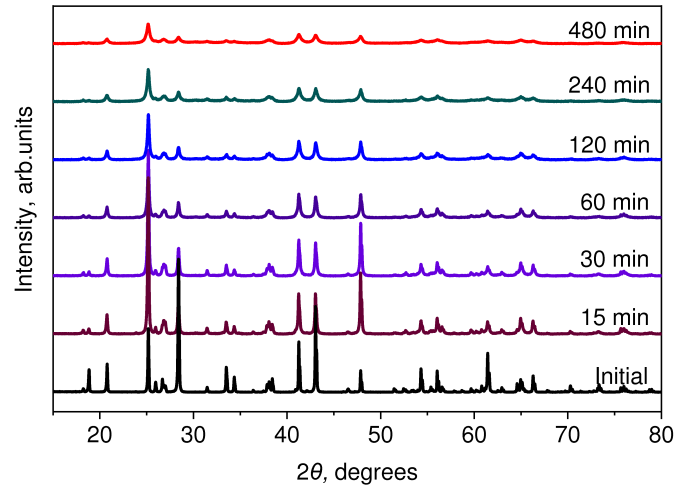
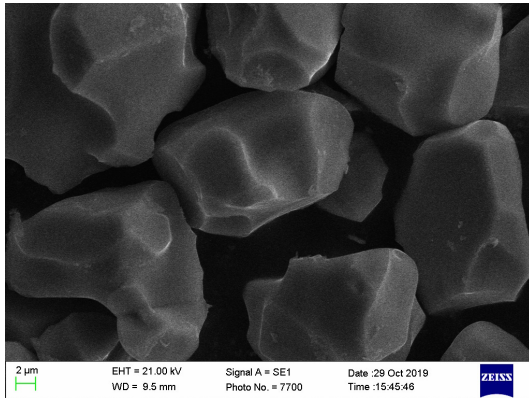


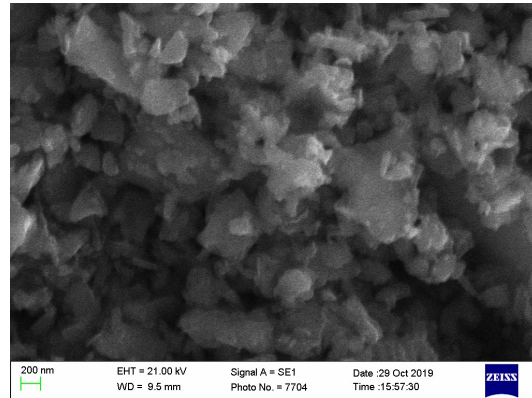
FIG. 1. X-ray diffraction patterns of the initial and milled Ti_3O_5 powders for 15 – 480 minutes

TABLE 1. Characteristics of the initial and milled Ti_3O_5 powders

Milling duration, min	CSR, nm	ϵ , %	Nanofraction volume, %	SSA (BET), m^2/g
Initial	—	0.02	—	0.120 ± 0.005
15	>100	0.15	1 ± 0.1	—
30	>100	0.06	2 ± 0.2	
60	100 ± 10	0.13	10 ± 1	
120	74 ± 10	0.09	20 ± 2	
240	60 ± 10	0.42	53 ± 5	17.194 ± 0.348
480	26 ± 10	0.49	81 ± 8	



(a)



(b)

FIG. 2. SEM images of powders: a) the initial microcrystal powder of Ti_3O_5 ; b) the nanocrystal powder of Ti_3O_5 after ball milling for 480 min

Figure 3 demonstrates the HRTEM micrographs of milled Ti_3O_5 powders by high-energy milling. According to HRTEM data, the powder consists of lamellar particles ranging in size from 20 nm to 1 μm (Fig. 3a). Regions with well crystallized structure are observed where the dimensions of blocks are 100 nm. In addition, a sufficiently large number of microcracks and distortions are observed. According to the EDX analysis carried out from a wide area, in addition to Ti, the powder contains zirconium Zr impurities (about 1 wt %) from the milling balls. According to the observed interplanar spacing, the phase corresponds to the Ti_3O_5 phase (Fig. 3b) with monoclinic structure (sp. gr. $C2/m$, PDF Number: 11-217).

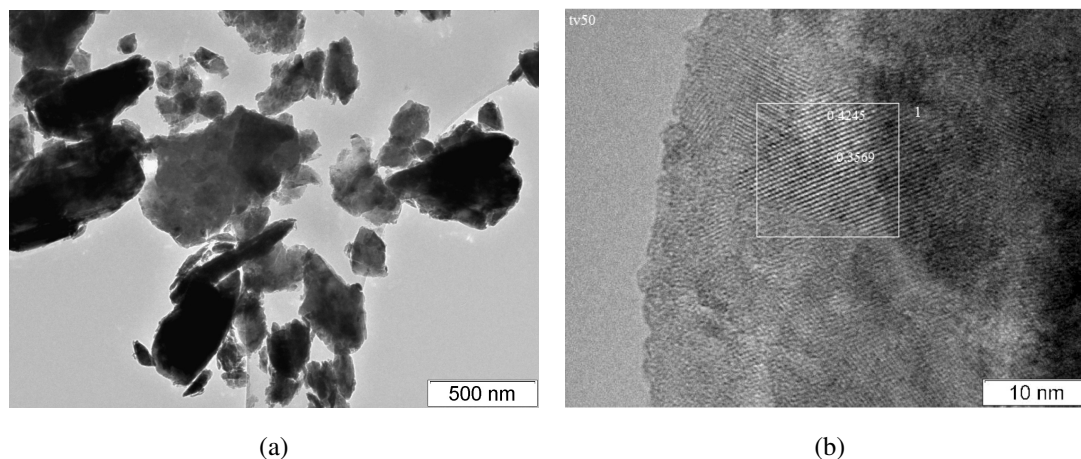


FIG. 3. HRTEM images of milled Ti_3O_5 nanocrystals: a) the powder consists of plate-like particles 10 nm – 1 μm in size; b) well crystallized structure, dimensions of blocks 100 nm, the observed interplanar spacings d_{hkl} correspond to Ti_3O_5 phase (PDF 11-217)

4. Conclusions

Thus, the effect of high impact loads on the crystal structure and stability of monoclinic titanium oxide Ti_3O_5 during high-energy ball milling was studied by X-ray powder diffraction. A full-profile analysis of the XRD spectra of milled Ti_3O_5 powders showed that high-energy ball milling does not lead to disordering or changing of stoichiometry, the structure remains monoclinic (sp. gr. $C2/m$), the phase composition and oxygen content does not changed. According to XRD pattern analysis reflections of milled powders are broadened due to the small particle size and microdeformations. The Williamson-Hall method was used to analyze the dependence of the reduced broadening of reflections on the length of the scattering vector s . It was found that milling leads to a decrease in CSR from 30 μm to 26 nm, an increase in microdeformations from 0.02 % for the initial powder to 0.49 % for the milled powder for 480 min, and the specific surface area increases from 0.1 to 17 m^2/g . The nanophase volume reaches only 81 % after milling for 480 min. According to the SEM and HRTEM data, coalescence of milled nanoparticles is observed, in addition, the particles are rigidly linked to each other and form particle agglomerates. Thus, the milling conditions indicated in this work make it possible to obtain nanosized titanium oxide Ti_3O_5 powder, and the monoclinic Ti_3O_5 phase (sp. gr. $C2/m$) is a thermodynamically stable phase.

References

- [1] Wang Y., Qin Y., et al. One-step synthesis and optical properties of blue titanium suboxide nanoparticles. *J. of Crystal Growth*, 2005, **282** (3–4), P. 402–406.
- [2] Valeeva A.A., Kostenko M.G. Stable Ti_9O_{10} nanophase grown from nonstoichiometric titanium monoxide TiO_y nanopowder. *Nanosystems: Phys. Chem. Math.*, 2017, **8** (6), P. 816–822.
- [3] Hauf C., Kniep R., Pfaff, G. Preparation of various titanium suboxide powders by reduction of TiO_2 with silicon. *J. of Materials Science*, 1999, **34** (6), P. 1287–1292.
- [4] Valeeva A.A., Nazarova S.Z., Rempel A.A. Influence of particle size, stoichiometry, and degree of long-range order on magnetic susceptibility of titanium monoxide. *Physics of the Solid State*, 2016, **58** (4), P. 771–778.
- [5] Kostenko M.G., Valeeva A.A., Rempel A.A. Octahedral Clusters in Various Phases of Nonstoichiometric Titanium Monoxide. *Mendeleev Communications*, 2012, **22** (5), P. 245–247.
- [6] Rempel A.A., Valeeva A.A. Thermodynamics of atomic ordering in nonstoichiometric transition metal monoxides. *Mendeleev Communications*, 2010, **20** (2), P. 101–103.
- [7] Bachina A.K., Popkov V.I., et al. Synthesis, Characterization and Photocatalytic Activity of Spherulite-like $r\text{-TiO}_2$ in Hydrogen Evolution Reaction and Methyl Violet Photodegradation. *Catalysts*, 2022, **12** (12), 1546.
- [8] Dorosheva I.B., Valeeva A.A., et al. Synthesis and Physicochemical Properties of Nanostructured TiO_2 with Enhanced Photocatalytic Activity. *Inorganic Materials*, 2021, **57** (5), P. 503–510.
- [9] Valeeva A.A., Dorosheva I.B., et al. Solar photocatalysts based on titanium dioxide nanotubes for hydrogen evolution from aqueous solutions of ethanol. *Int. J. of Hydrogen Energy*, 2021, **46** (32), P. 16917–16924.

- [10] Rempel A.A., Valeeva A.A. Nanostructured titanium dioxide for medicinal chemistry. *Russian Chemical Bulletin*, 2019, **68** (12), P. 2163–2171.
- [11] Dorosheva I.B., Valeeva A.A., Rempel A.A. Sol-gel synthesis of nanosized titanium dioxide at various pH of the initial solution. *AIP Conference Proceedings*, 2017, **1886**, 020006.
- [12] Rempel A.A., Kuznetsova Y.V., et al. High Photocatalytic Activity Under Visible Light of Sandwich Structures Based on Anodic TiO_2/CdS Nanoparticles/Sol-Gel TiO_2 . *Topics in Catalysis*, 2020, **63** (1–2), P. 130–138.
- [13] Popkov V.I., Bachina A.K., et al. Synthesis, morphology and electrochemical properties of spherulite titania nanocrystals. *Ceramics Int.*, 2020, **46** (14), P. 24483–24487.
- [14] Vasilevskaia A.K., Popkov V.I., Valeeva A.A., Rempel A.A. Formation of nonstoichiometric titanium oxides nanoparticles Ti_nO_{2n-1} upon heat-treatments of titanium hydroxide and anatase nanoparticles in a hydrogen flow. *Russian J. of Applied Chemistry*, 2016, **89** (8), P. 1211–1220.
- [15] Yoshimatsu K., Sakata O., Ohtomo A. Superconductivity in Ti_4O_7 and $\gamma-Ti_3O_5$ films. *Scientific Reports*, 2017, **7** (1), P. 1–7.
- [16] Yang S., Zhang L., et al. A novel carbon thermal reduction approach to prepare recorded purity $\beta-Ti_3O_5$ compacts from titanium dioxide and phenolic resin. *J. of Alloys and Compounds*, 2021, **853**, 157360.
- [17] Tanaka K., Nasu T., et al. Structural Phase Transition between $\gamma-Ti_3O_5$ and $\delta-Ti_3O_5$ by Breaking of a One-Dimensionally Conducting Pathway. *Crystal Growth & Design*, 2014, **15** (2), P. 653–657.
- [18] Rempel A.A., Valeeva A.A., Vokhmintsev A.S., Weinstein I.A. Titanium dioxide nanotubes: Synthesis, structure, properties and applications. *Russian Chemical Reviews*, 2021, **90** (11), P. 1397–1414.
- [19] Valeeva A.A., Rempel A.A., et al. Nonstoichiometry, structure and properties of nanocrystalline oxides, carbides and sulfides. *Russian Chemical Reviews*, 2021, **90** (51), P. 601–626.
- [20] Valeeva A.A., Nazarova S.Z., Rempel A.A. Nanosize effect on phase transformations of titanium oxide Ti_2O_3 . *J. of Alloys and Compounds*, 2019, **817**, 153215.
- [21] Valeeva A.A., Nazarova S.Z., et al. Effects of high mechanical treatment and long-term annealing on crystal structure and thermal stability of Ti_2O_3 nanocrystals. *RSC Advances*, 2020, **10** (43), P. 25717–25720.
- [22] Indris S., Amade R., et al. Preparation by High-Energy Milling, Characterization, and Catalytic Properties of Nanocrystalline TiO_2 . *The J. of Physical Chemistry B*, 2005, **109** (49), P. 23274–23278.
- [23] Melchakova O.V., Pechishcheva N.V., Korobitsyna A.D. Mechanically activated rutile and its sorption properties with regard to gallium and germanium. *Tsvetnye Metally*, 2019, **1**, P. 32–39.
- [24] Valeeva A.A., Schröttner H., Rempel A.A. Fragmentation of disordered titanium monoxide of stoichiometric composition TiO . *Russian Chemical Bulletin*, 2014, **63** (12), P. 2729–2732.
- [25] Valeeva A.A., Nazarova S.Z., Rempel A.A. Size effect on magnetic susceptibility of titanium monoxide nanocrystals. *Physica Status Solidi B*, 2016, **253** (2), P. 392–396.
- [26] Uzunova-Bujnova M., Dimitrov D., et al. Effect of the mechanoactivation on the structure, sorption and photocatalytic properties of titanium dioxide. *Materials Chemistry and Physics*, 2008, **110** (2–3), P. 291–298.
- [27] Ordinarov D.P., Pechishcheva N.V., et al. Nanosized Titania for Removing Cr(VI) and As(III) from Aqueous Solutions. *Russian J. of Physical Chemistry A*, 2022, **96** (11), P. 2408–2416.
- [28] Hall W.H. X-Ray Line Broadening in Metals. *Proceedings of the Physical Society*, 1949, **62**, P. 741–743.

Submitted 5 October 2022; accepted 24 October 2022

Information about the authors:

Albina A. Valeeva – Institute of Solid State Chemistry, Ural Branch of the Russian Academy of Sciences, 620108, Ekaterinburg, Russia; ORCID 0000-0003-1656-732X; anibla_v@mail.ru

Irina B. Dorosheva – Ural Federal University, 620002, Ekaterinburg, Russia; Institute of Metallurgy, Ural Branch of the Russian Academy of Sciences, 620016 Ekaterinburg, Russia; ORCID 0000-0001-9229-6758; dorosheva1993@mail.ru

Anna A. Sushnikova – Institute of Metallurgy, Ural Branch of the Russian Academy of Sciences, 620016 Ekaterinburg, Russia; ORCID 0000-0002-7604-5673; sushnikova.ann@gmail.com

Conflict of interest: the authors declare no conflict of interest.